MICROCOPY RESOLUTION TEST CHART
NATIONAL BUREAU OF STANDARDS-1963-A

IVE HIGH FREQUENCY TECHNIQUES FOR UHF AND ABOVE ANTENNAS
Quarterly Report - 1 November 1976 to 31 January 1977

W.D. Burnside
R.G. Kouyoumjian
R.J. Marhefka
R.C. Rudduck
C.H. Walter

The Ohio State University

ElectroScience Laboratory

83 08 29 044

DTIC
SELECTED
SEP 06 198
E

NOTICES

When Government drawings, specifications, or other data are used for any purpose other than in connection with a definitely related Government procurement operation, the United States Government thereby incurs no responsibility nor any obligation whatsoever, and the fact that the Government may have formulated, furnished, or in any way supplied the said drawings, specifications, or other data, is not to be regarded by implication or otherwise as in any manner licensing the holder or any other person or corporation, or conveying any rights or permission to manufacture, use, or sell any patented invention that may in any way be related thereto.

SECURITY CLASSIFICATION OF THIS PAGE *(When Data Entered)*

REPORT DOCUMENTATION PAGE	READ INSTRUCTIONS BEFORE COMPLETING FORM

1 REPORT NUMBER	2 GOVT ACCESSION NO. *AP32 097*	RECIPIENT'S CATALOG NUMBER

4 TITLE *(and Subtitle)*	5 TYPE OF REPORT & PERIOD COVERED
ASYMPTOTIC HIGH FREQUENCY TECHNIQUES FOR UHF AND ABOVE ANTENNAS	Second Quarterly Report 11/1/76 - 1/31/77
	6 PERFORMING ORG REPORT NUMBER ESL 4508-2

7 AUTHOR(s)	8 CONTRACT OR GRANT NUMBER(s)
W.D. Burnside, R.G. Kouyoumjian, R.J. Marhefka, R.C. Rudduck, C.H. Walter	N00123-76-C-1371

9 PERFORMING ORGANIZATION NAME AND ADDRESS	10 PROGRAM ELEMENT PROJECT TASK AREA & WORK UNIT NUMBERS
The Ohio State University ElectroScience Laboratory, Department of Electrical Engineering Columbus, Ohio 43212	Project N00953/6/009121

11 CONTROLLING OFFICE NAME AND ADDRESS	12 REPORT DATE
Naval Regional Procurement Office Long Beach, California 90822	February 1977
	13 NUMBER OF PAGES 22

14 MONITORING AGENCY NAME & ADDRESS *(if different from Controlling Office)*	15 SECURITY CLASS. *(of this report)*
	Unclassified
	15a DECLASSIFICATION DOWNGRADING SCHEDULE

16 DISTRIBUTION STATEMENT *(of this Report)*

Approved for public release;
distribution unlimited.

17 DISTRIBUTION STATEMENT *(of the abstract entered in Block 20, if different from Report)*

18 SUPPLEMENTARY NOTES

19 KEY WORDS *(Continue on reverse side if necessary and identify by block number)*

Computer code	Aperture integration	Cylinders
Algorithm	Slope diffraction	
Geometrical Theory of Diffraction	Vertex diffraction	
Far Field Pattern	Flat plates	
Reflector Antenna	Boxes	

20 ABSTRACT *(Continue on reverse side if necessary and identify by block number)*

The overall scope of the program on Contract No. N00123-76-C-1371 between The Ohio State University ElectroScience Laboratory and the Naval Electronics Laboratory Center is to develop the necessary theory, algorithms and computer codes for simulating antennas at UHF and above in a complex ship environment. The work consists of a) basic scattering code development, b) reflector antenna code development and c) basic studies to support items a) and b). This report describes the progress in each of these three areas for the period 1 November 1976 to 31 January 1977.

DD `FORM 1 JAN 73` **1473** EDITION OF 1 NOV 65 IS OBSOLETE

TABLE OF CONTENTS

I.   INTRODUCTION

This report describes the work done on Contract No. N00123-76-C-1371 for the period 1 November 1976 to 31 January 1977.

The overall program is divided into three areas. These are 1) basic scattering code development, 2) reflector antenna code development and 3) basic theoretical studies to support the first two areas. The following sections describe the progress made during the second quarter in each of the three areas mentioned above.

II.   PROGRAM SCOPE

The scope of the work under Contract No. N00123-76-C-1371 is to develop the necessary theory, algorithms and computer codes for simulating antennas at UHF and above in a complex ship environment. A milestone chart for the total program, which extends over a three year period, is shown in Table I. A more detailed breakdown of the effort planned for the first year is shown in Table II. The following sections describe the progress made during the second quarter of the program in Table II.

III.   BASIC SCATTERING CODE DEVELOPMENT

The purpose of this section is to describe the present status of the basic scattering code development for the analysis of antennas in a complex shipboard environment. The Geometrical Theory of Diffraction (GTD) is being used to develop algorithms to solve for the scattering from basic plate and cylinder structures. These simple components can then be combined to form box-like structures and finite elliptic cylinders that can represent various component structures of a ship. The algorithms are being implemented into a user-oriented computer code.

In this period the multiple plate scattering code has been improved and tested. This multiplate code allows a number of N sided flat plates to be placed in proximity to each other such that they can form arbitrary box-shaped structures. Some improvements have been made in the algorithms to help the accuracy and efficiency of the computer codes. For example, the algorithm for finding reflected fields from flat surfaces has been improved by a more efficient image theory solution. Also, the algorithm used to find the incident field needed for the slope diffracted field has been improved such that it will allow use of a more general source.

The validity of the multiple plate scattering code is being tested by comparing the results against experimental measurements. The first comparisons were made with a dipole antenna near two plates forming a convex edge (roof-like structure) as illustrated in the insert of Fig. 1. The GTD and measured results are compared in Figs. 1-5 for various pattern cuts and polarizations as illustrated in the figures. The agreement is very good in all cases.

1

TABLE I

MILESTONE CHART FOR TOTAL PROGRAM

Task

Time

	1st year	2nd year	3rd year

1. BASIC SCATTERING CODE DEVELOPMENT

a. Flat plate, box and cylinder independently analyzed for far field effects

b. Coupled solution for flat plate, box and cylinder - far field

c. Near field analysis of coupled structure including coupled antennas.

2. REFLECTOR ANTENNA CODE DEVELOPMENT

a. General reflector, no blockage, far field

b. General reflector, no blockage, near field

c. General reflector with scattering from feed, supports, subreflectors and ship structure

------- Theoretical development

——— Formulate algorithms and write and implement computer codes

2

TABLE II

ASYMPTOTIC HIGH FREQUENCY TECHNIQUES
FOR UHF AND ABOVE ANTENNAS

FIRST YEAR WORK PLAN

	1st Quarter		2nd Quarter
Topic	Task		Task
1. Basic Scattering Code Development			
	FF Flat Plate (T,A)		FF Box (T,A)
	FF Cylinder (T,A)		FF Cylinder (T,A)
2. Reflector Antenna Code Development			
	General reflector		General reflector
	FF w/o blockage (T)		FF w/o blockage (T)
3. Theoretical Studies			
	Slope Diffraction (T)		Vertex Diffraction (T)

T - Theory
A - Algorithm
U - Code with User's Manual

3

TABLE II (Contd.)

**ASYMPTOTIC HIGH FREQUENCY TECHNIQUES
FOR UHF AND ABOVE ANTENNAS**

FIRST YEAR WORK PLAN

|	3rd Quarter	4th Quarter
Topic	Task	Task
1. Basic Scattering Code Development		
	FF Box (A,U)	FF Box (U)
	FF Cylinder (A,U)	FF Cylinder (U)
	Plate Box Cylinder } Coupled FF (T,A)	Plate Box Cylinder } Coupled FF (T,A)
2. Reflector Antenna Code Development		
	General Reflector	General Reflector
	FF w/o blockage (T,A)	FF w/o blockage (A,U)
	General Reflector	General Reflector
	NF w/o blockage (T)	NF w/o blockage (T)
3. Theoretical Studies		
	Vertex Diffraction(T)	Vertex Diffraction(T)

4
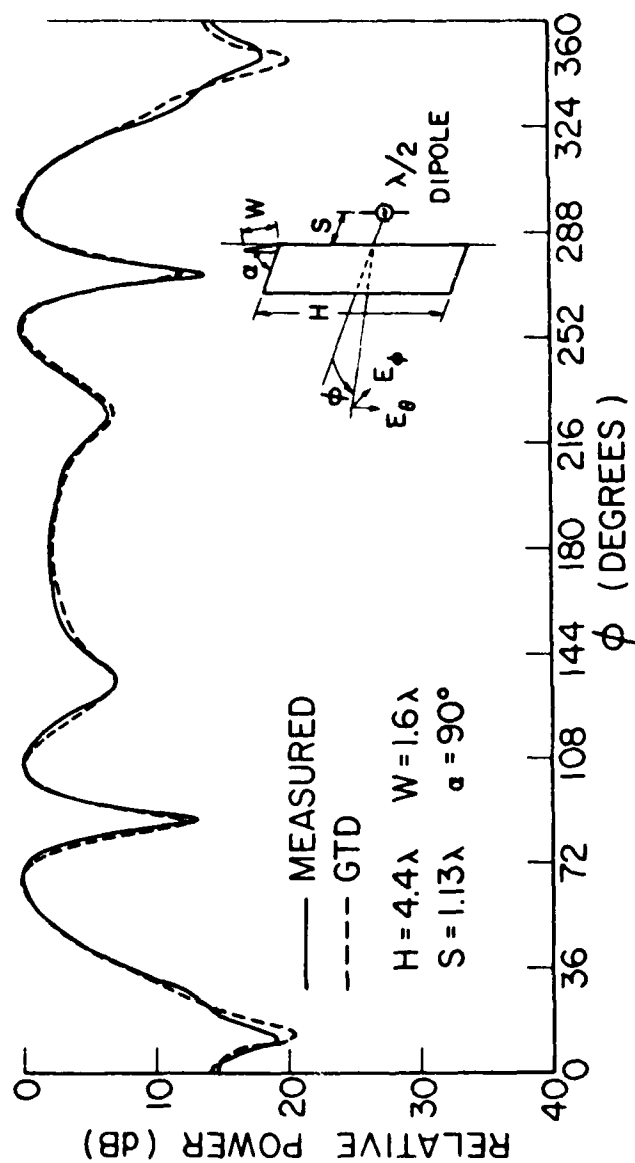
Fig. 1. Comparison of the measured and calculated E_θ radiation pattern of a dipole near a roof-like structure in the indicated plane.
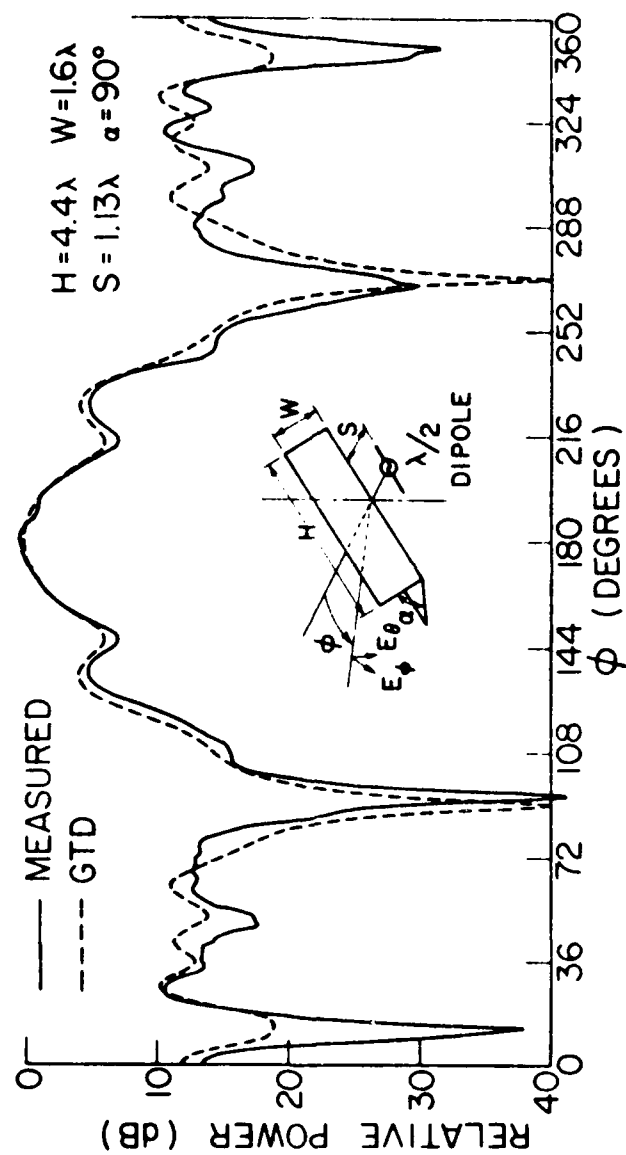
5

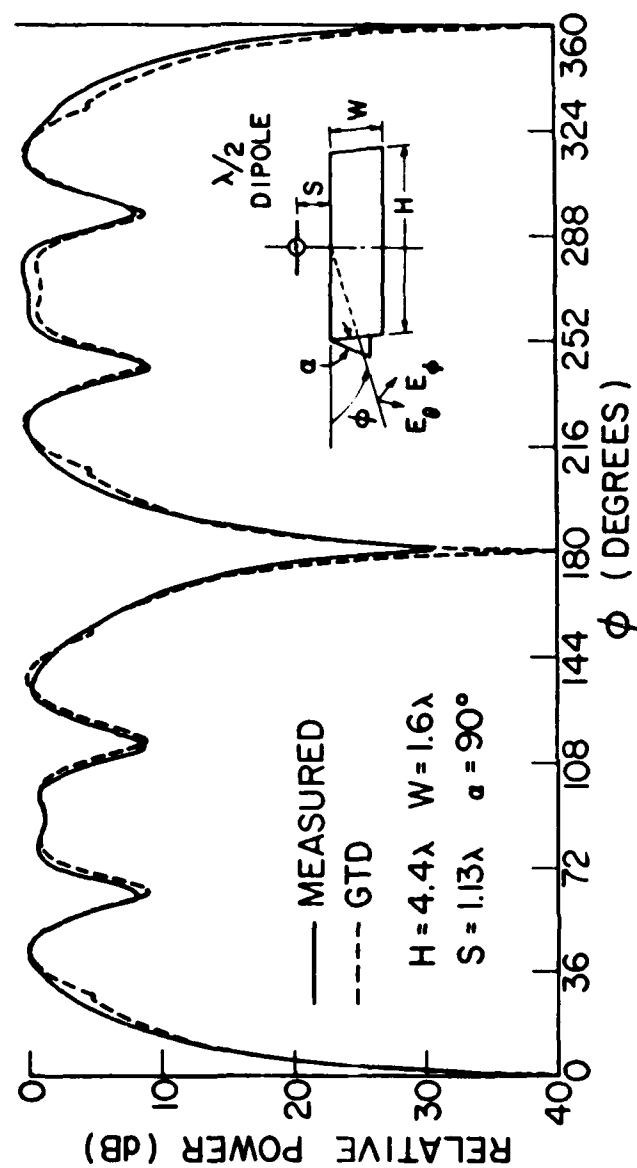Fig. 2. Comparison of the measured and calculated E_j radiation pattern of a dipole near a roof-like structure.
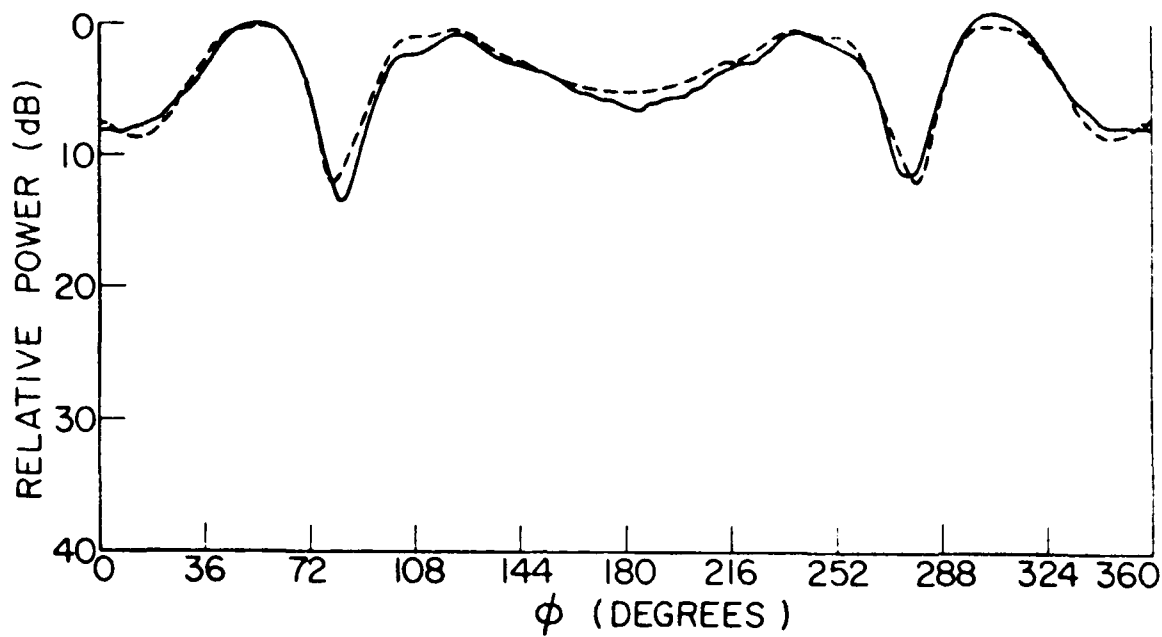
Fig. 3. Comparison of the measured and calculated E_ϕ radiation pattern of a dipole near a roof-like structure.

7
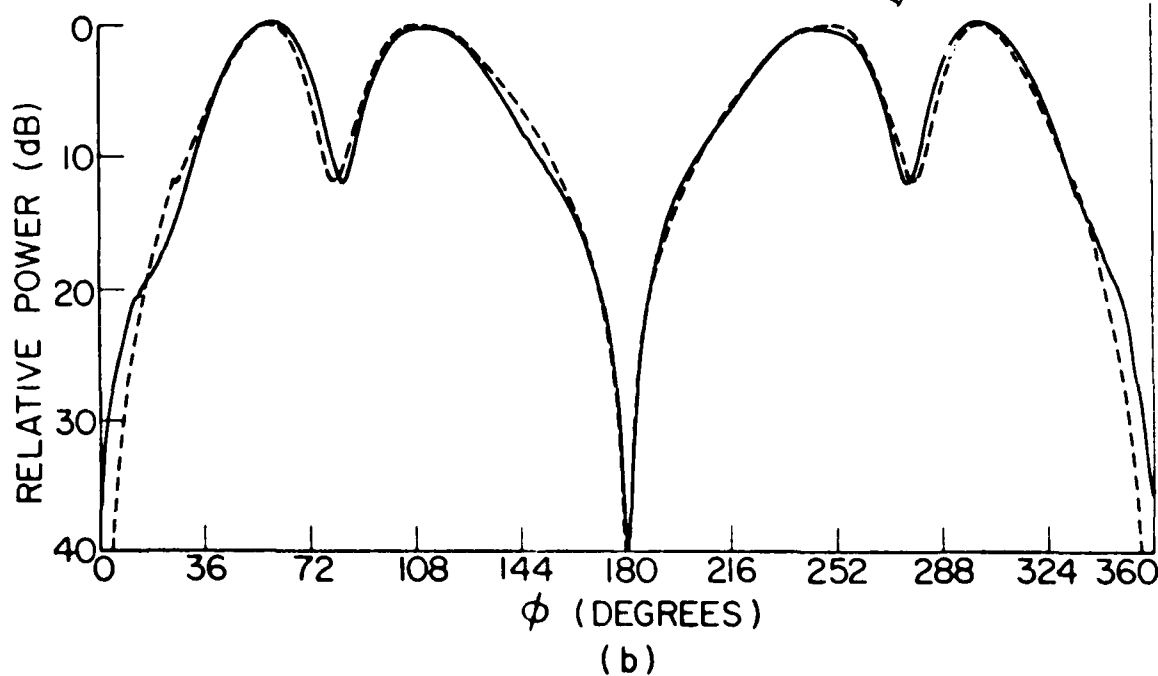
Fig. 4.   Comparison of the measured and calculated radiation
pattern for a) E_θ and b) E_ϕ polarizations.

8

Fig. 5. Comparison of the measured and calculated radiation
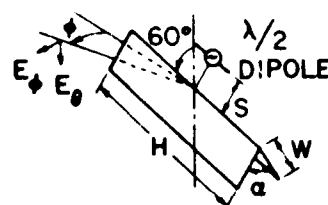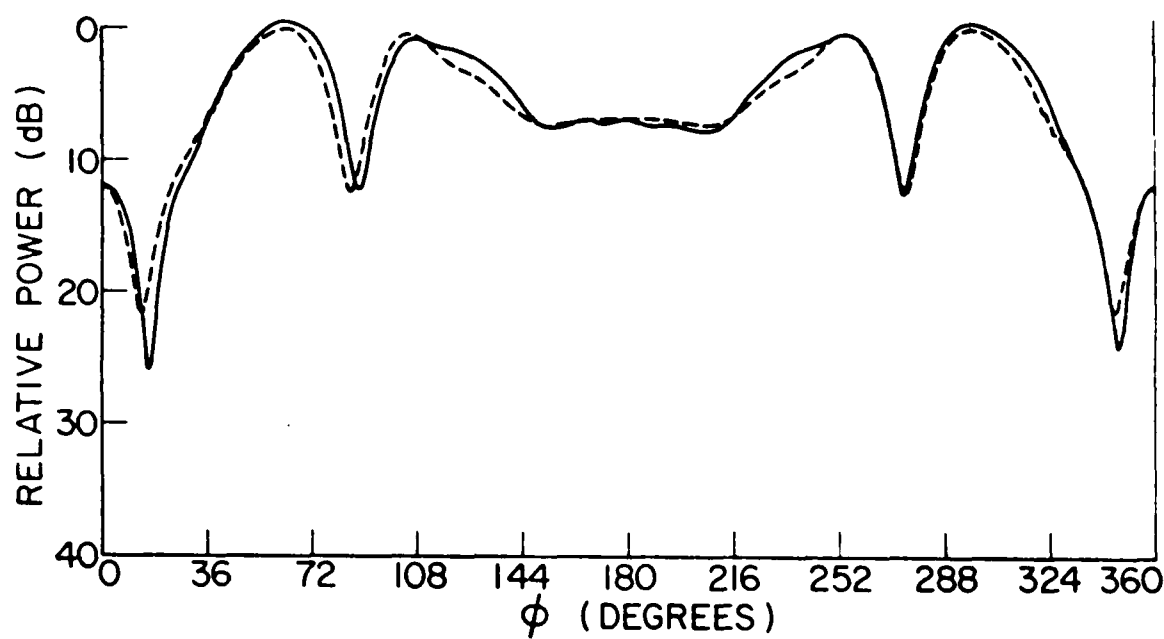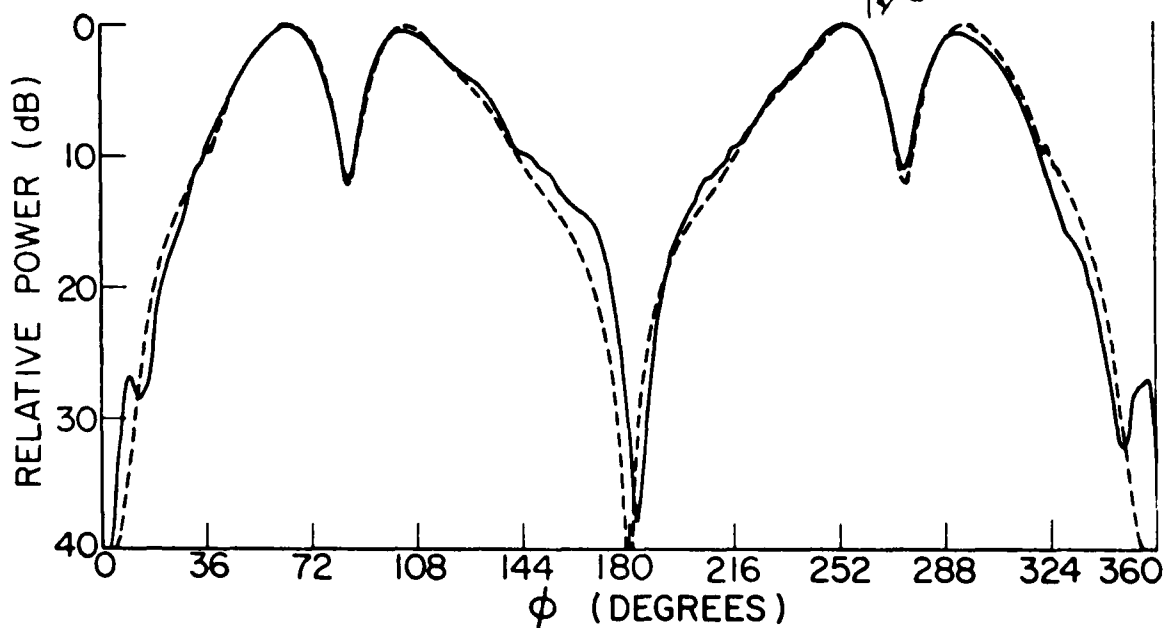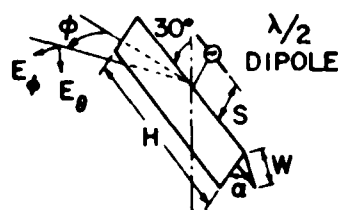pattern for a) E_θ and b) E_ϕ polarizations.

9

One of the reasons for this excellent agreement in all the pattern cuts is the use of newly developed empirical corner and slope-corner diffraction coefficients (vertex diffraction). To show how important these terms are in finding volumetric patterns, Figs. 6 and 7 show GTD results for the above roof-shaped structure without the corner diffraction terms compared against measured results. The discontinuities shown in the patterns result from the regular edge diffraction and slope diffraction terms "falling off" at the fini__ limits of the edges of the plates. The empirical corner and slope-corner diffraction terms smooth out these discontinuities as was previously shown for these two cases in Figs. 2 and 3, respectively.

It must be cautioned that these newly developed empirical corner diffraction terms have not been put on a firm rigorous foundation as yet. This should be done in order to have complete confidence in the results for all possible applications. The primary justification up to this point is the experimental agreement. It is felt that this is sufficient evidence to continue their use at the present time.
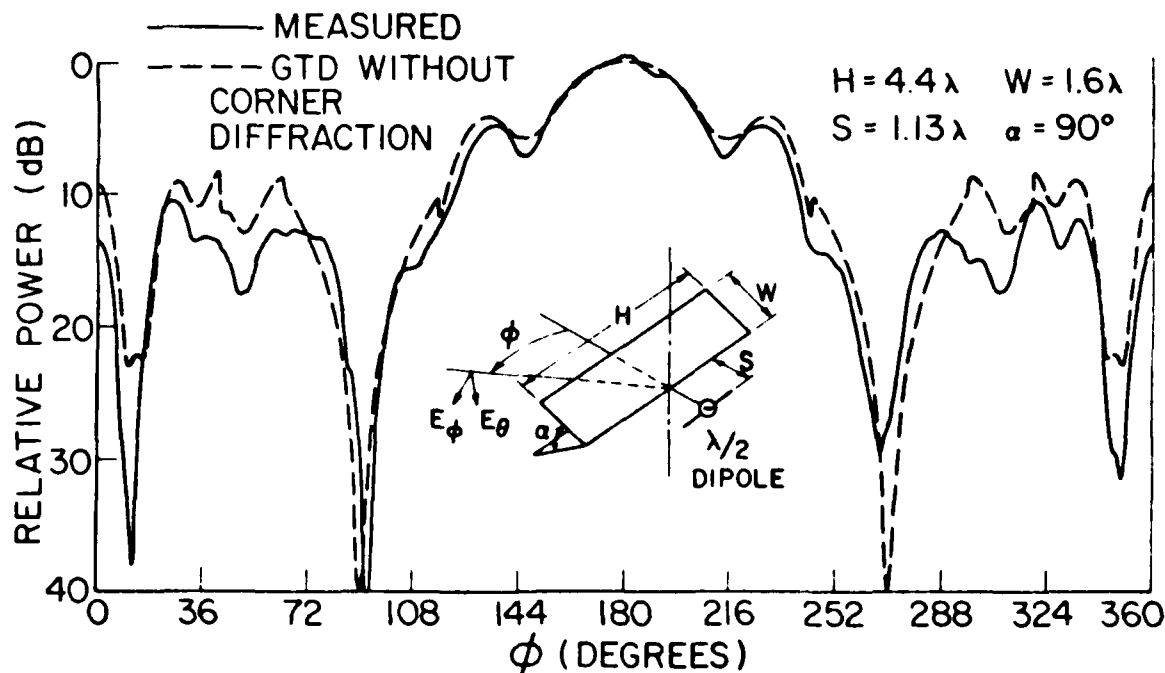

Fig. 6. Comparison of the measured and calculated (without corner diffraction) E_t radiation pattern (refer to Fig. 2).
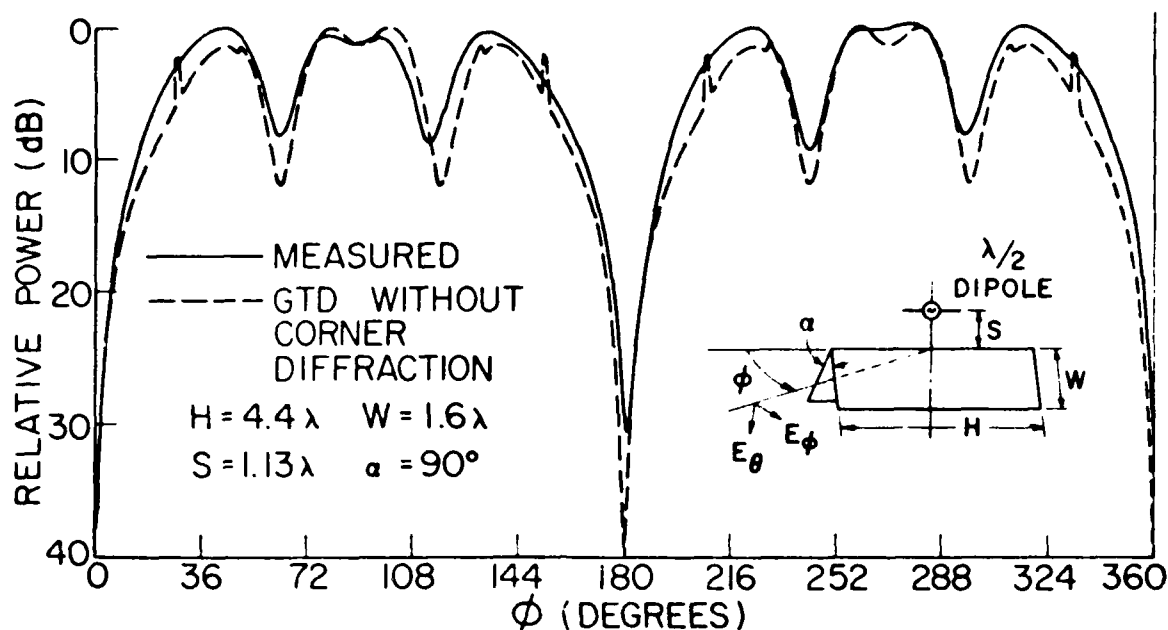
10

Fig. 7. Comparison of measured and calculated (without
         corner diffraction) E_ϕ radiation pattern
         (refer to Fig. 3).

   The scattering code also has been tested on a box-shape as illustrated
in the insert of Fig. 8. The scattering code result without the corner
diffraction terms is compared with measured results in Fig. 8a. Note
that the empirical corner diffraction terms are again needed to obtain
a continuous field pattern. This is shown in Fig. 8b which compares the
scattering code result with the empirical corner diffraction coefficient
included against measured results. Comparison between the GTD with
corner diffraction and measured results are shown for two other cases in
Figs. 9 and 10. The good agreement obtained again confirms the validity
of the theoretical results.

   The basic scattering code for a finite elliptic cylinder also has
been investigated during this period. In particular, the diffraction
mechanisms used to model the junction between the flat plate endcaps and
the curved elliptic cylinder surface have been studied. A curved edge
dyadic diffraction coefficient developed by Kouyoumjian and Pathak[1] is
used to find the fields scattered from the edges. In general, there are
four points of diffraction around one of these elliptic rims for a given
observation direction. Previously, a search technique was used to locate
these points. However, this proved to be a very time consuming means of
locating the points of diffraction. A faster method has been developed
for finding these points by numerically solving for the roots of an
eighth order polynomial with coefficients that are a function of the
elliptic rim parameters and observation direction. This is essentially
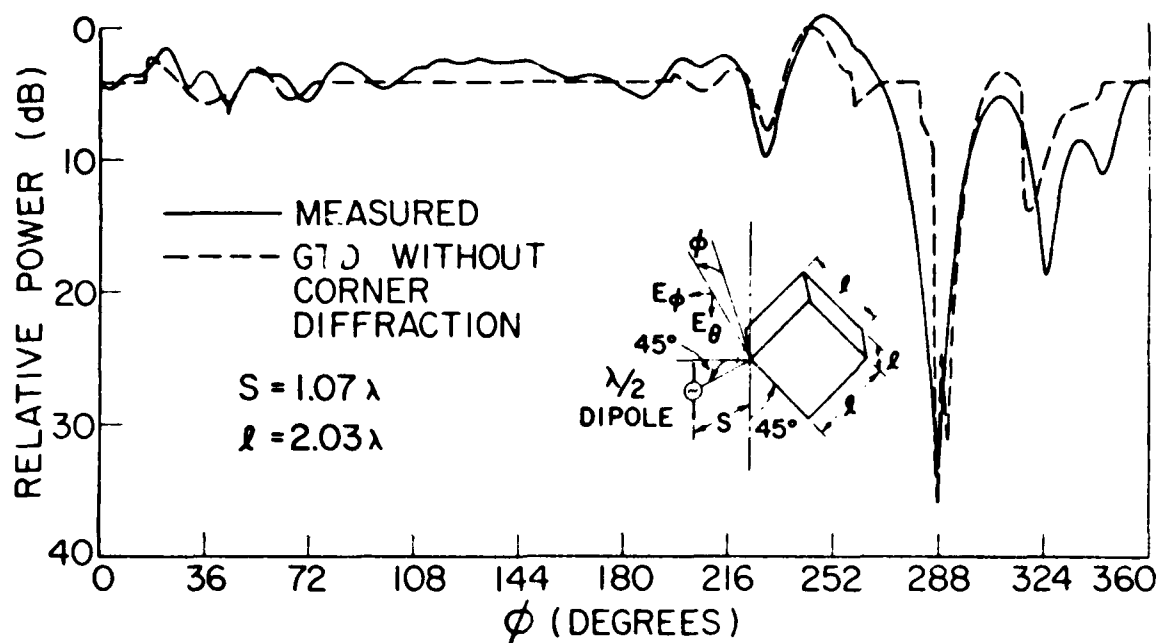
11

Fig. 8a.   Comparison of measured and calculated (without corner
            diffraction) E_θ radiation pattern for a dipole near
            a box in the indicated plane.
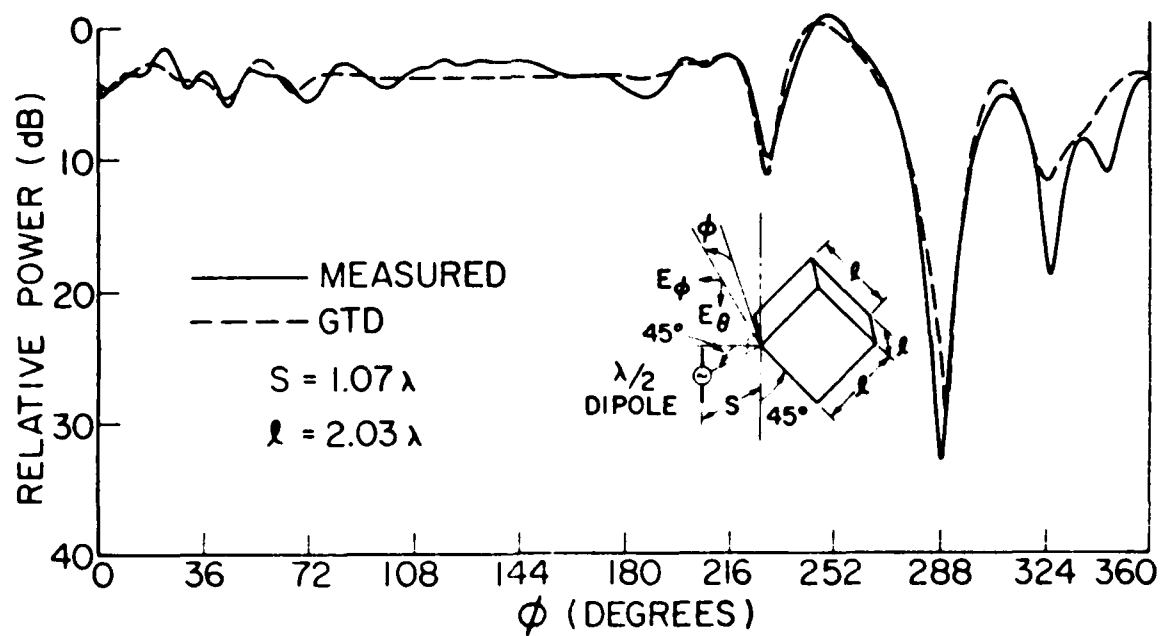

Fig. 8b.   Comparison of measured and calculated E_ϕ radiation
            pattern for a dipole near a box in the indicated
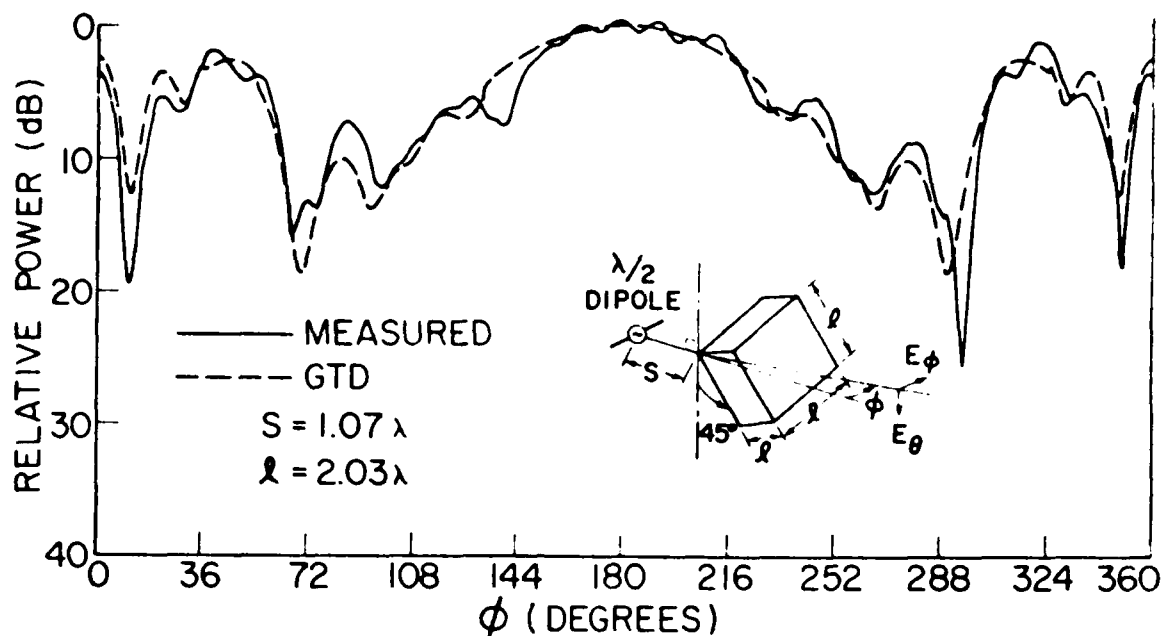   plane.

Fig. 9. Comparison of measured and calculated E_ϕ radiation
         pattern for a dipole near a box.

an exact solution of the diffraction points within the accuracy of the
algorithms for the numerical polynomial solution routines. The speed
of finding the diffraction points has been increased by a factor of 3.75
and consequently the overall program speed has been improved by a factor
of approximately 2. The computer storage needed for the program also
has been reduced in the process. Further improvements in the scattering
code are under investigation.

        In the next period, the scattering code for the plates and box-
shaped structures will be completed. It will be delivered to NELC
early in the fourth quarter. This early delivery of the first version
of the scattering code will allow for inputs from NELC on improvements
of the usefulness of subsequent scattering codes.

        The scattering code for the isolated finite elliptic cylinder will
be improved and tested as has been done for the plate-box code. When
this is completed the scattering code for the cylinder will be combined
with the plate-box code, but, it will not contain box-cylinder inter-
actions in this first combined code. This combined scattering code will
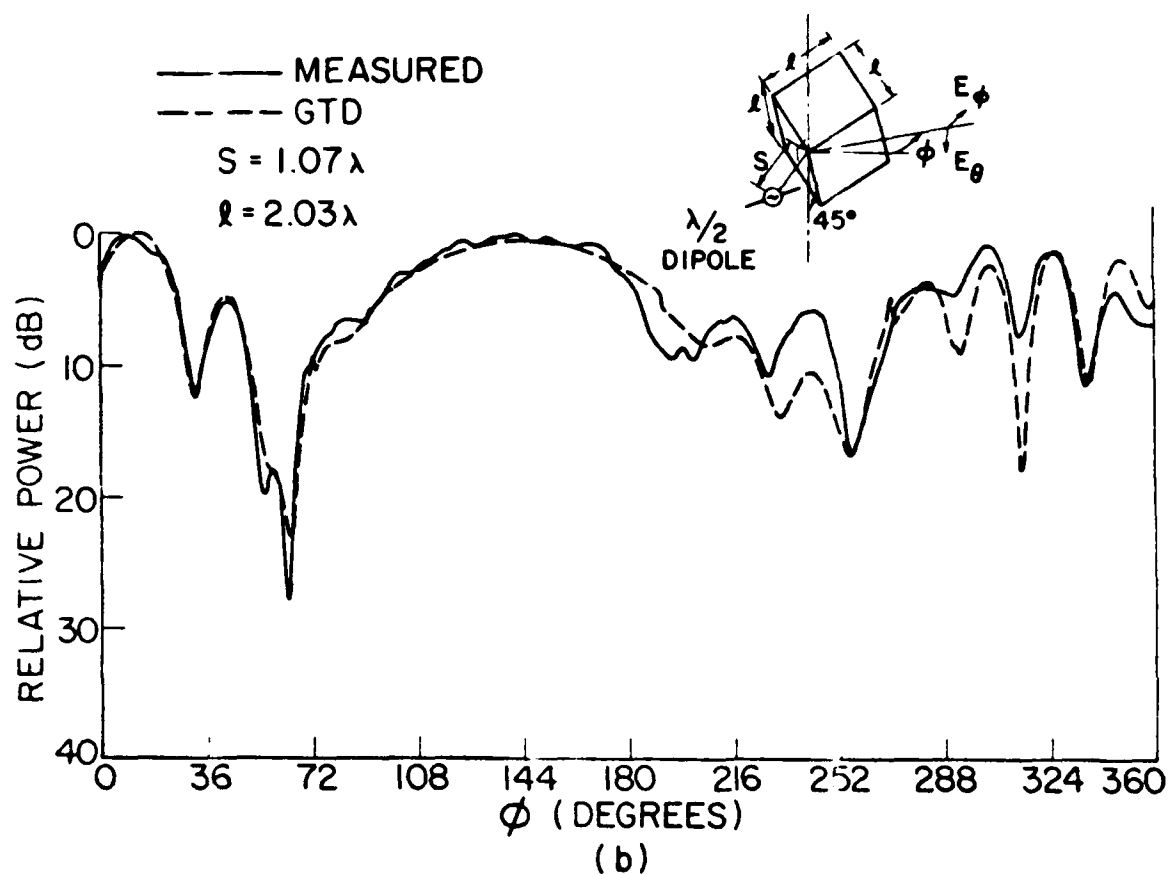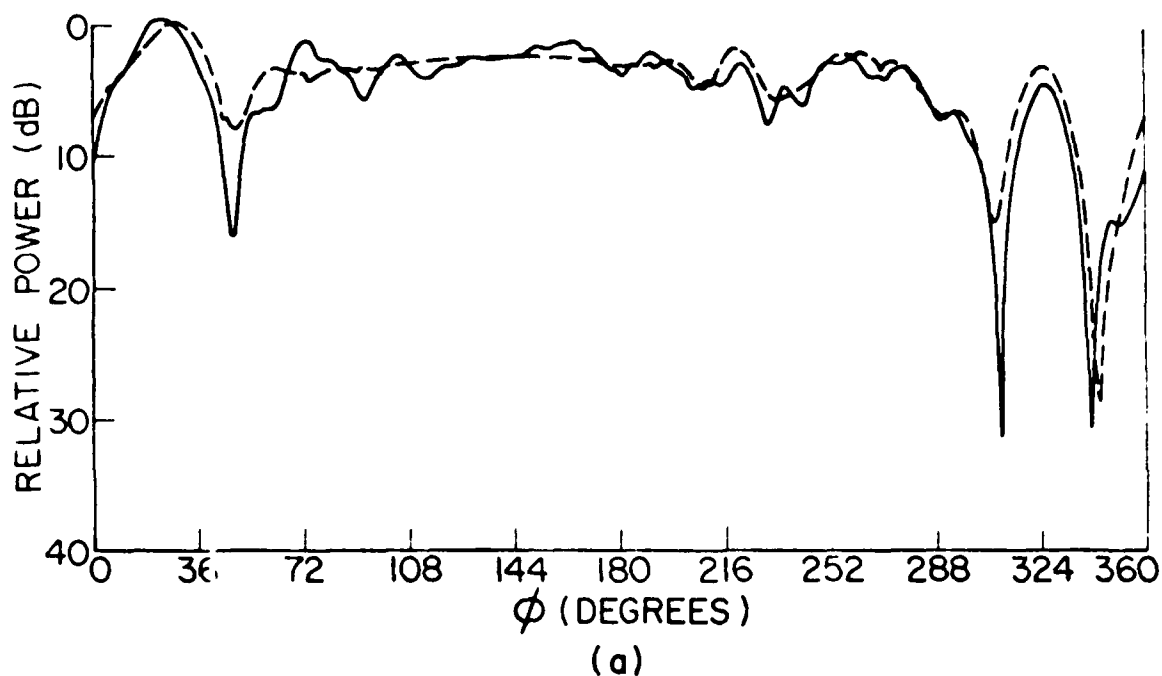be delivered sometime at the end of the fourth quarter along with a users
manual.

Fig. 10. Comparison of measured and calculation radiation
pattern, a) E_θ and b) E_ϕ.

14

This final code for the first year will allow field pattern com-
putations for isolated plates, boxes, finite elliptic cylinders, and a
psuedo combination of both without box-cylinder interactions. The theory
for the coupled solution that will include the dominate interactions for
the box-cylinder far field patterns will be under investigation for the
remainder of this contract year.

IV.   REFLECTOR ANTENNA CODE DEVELOPMENT

The purpose of the present effort is to develop a user-oriented
computer program package by which the far field pattern of a typical
Navy reflector antenna can be calculated. Feed blockage and scattering
effects are not included in this phase. These will be included later
(see Table I).

The theoretical approach 'or computing the far field pattern of the
general reflector is based on a combination of the Geometrical Theory of
Diffraction (GTD) and Aperture Integration (AI) techniques. AI will be
used to compute the main beam and near sidelobes; GTD will be used to
compute the wide-angle sidelobes and the backlobes. To implement the
computer algorithms based on these theories, efficient ways are needed
to handle calculations involving the feed pattern and the reflector
geometry. It is planned to treat the geometry of the reflector rim by
using best-fit elliptical or linear segments.

Since the majority of Navy reflector antennas have parabolic sur-
faces, only the class of parabolic surfaces will be implemented in the
computer code. The code for the reflector geometry will be flexible
enough to include off-set fed reflectors and general reflector rim shapes
such as elliptical and rectangular with chopped corners.

An efficient way to handle AI is necessary because of its time-
consuming nature for electrically large reflectors. Fortunately, AI is
needed only for the main beam and near sidelobe regions of the pattern.
GTD is very efficient for calculating most of the pattern. Two techni-
ques are being implemented to provide efficient AI: the polynomial-fit
method for the feed pattern and the use of overlapping rectangular sub-
apertures for the two-dimensional numerical integration required to cal-
culate the far field pattern.

The polynomial-fit method is used to obtain an analytic fit for
each measured pattern cut of the volumetric feed pattern. This method
provides a computationally efficient way of calculating the aperture
field without requiring large amounts of computer storage for the mea-
sured feed pattern. Only relatively few coefficients need to be stored
for essentially complete feed pattern information. Furthermore, the
polynomial-fit method has the advantages of flexibility and simplicity
for general feed patterns. No cut-and-try procedures are needed; the
polynomial coefficients can be computed automatically from the measured
feed pattern input.

As reported in the previous Quarterly report, computer subroutines were developed to provide a polynomial curve-fit for measured feed patterns. This method was demonstrated for typical sum and difference patterns. Further improvement was made this quarter for fitting measured feed patterns in the spillover region, i.e., where the feed radiation is not reflected by the reflector. At the low field levels encountered in the spillover region, a piecewise linear approximation was found to be a better representation for this part of the feed pattern. Thus the computer subroutines were modified to use a combination of polynomial-fit for the major part of the feed pattern and a piecewise linear fit for most of the spillover region of the pattern.

The polynomial-fit method is based on approximating a measured feed pattern by

$$(1) \qquad f(\psi) = \sum_{\iota=1}^{N} B_\iota \left(\frac{\psi - \psi_1}{\psi_2 - \psi_1} \right)^m$$

The polynomial fit is obtained for $\psi_1 \leq \psi \leq \psi_2$ as shown in Fig. 11.

The feed pattern may be a symmetrical sum pattern (even terms only), a symmetrical difference pattern (odd terms only), or a general unsymmetric pattern (both even and odd terms). Thus, in Eq. (1)

$$(2) \qquad m = \begin{cases} 2\iota - 2 & \text{even terms only} \\ 2\iota - 1 & \text{odd terms only} \\ \iota - 1 & \text{both odd and even terms} \end{cases}$$

For a symmetrical sum pattern (even terms only) and with the usual value of $\psi_1 = 0$:

$$(3) \qquad f(\psi) = B_1 + B_2 \left(\frac{\psi}{\psi_2} \right)^2 + \cdots + B_N \left(\frac{\psi}{\psi_2} \right)^{2N-2}$$

where N is the number of measured feed pattern values that are fitted. Thus substituting the N known feed values $f(\psi_{xi})$ into Eq. (3) gives N equations and N unknown coefficients:

$$(4) \qquad f(0) = B_1$$
$$f(\psi_{x2}) = B_1 + B_2 \left(\frac{\psi_{x2}}{\psi_2} \right)^2 + \cdots + B_N \left(\frac{\psi_{x2}}{\psi_2} \right)^{2N-2}$$
$$\vdots$$
$$f(\psi_{xN}) = B_1 + B_2 \left(\frac{\psi_{xN}}{\psi_2} \right)^2 + \cdots + B_N \left(\frac{\psi_{xN}}{\psi_2} \right)^{2N-2}$$
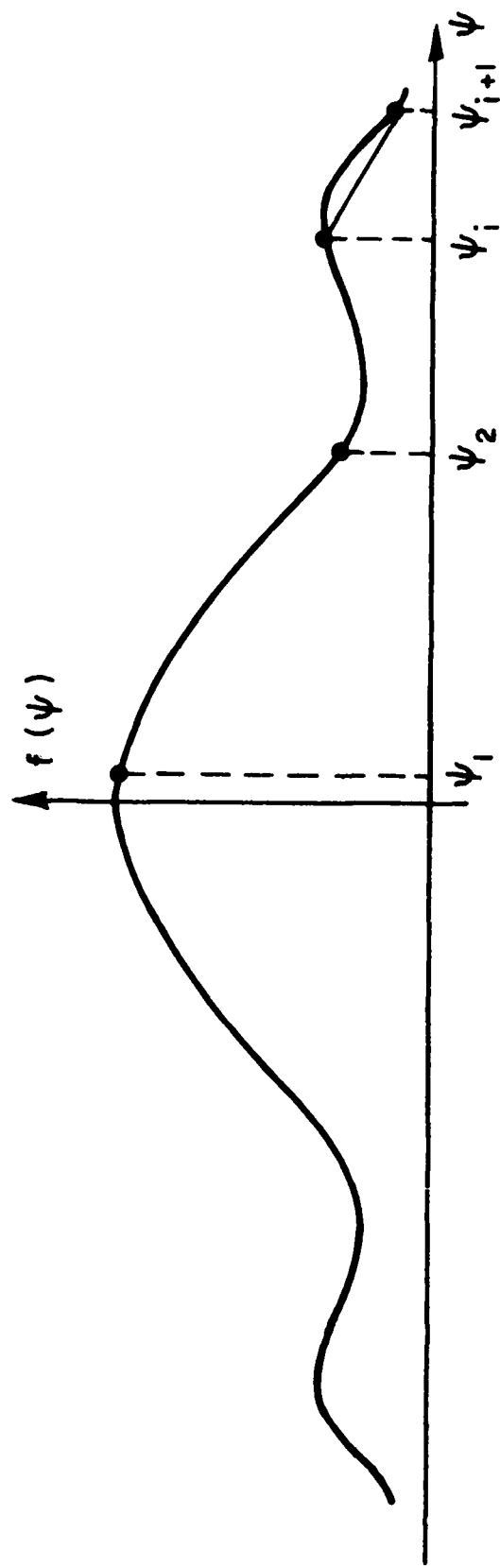
Fig. 11. Polynomial-fit and piece-wise linear approximation for feed patterns.

7

By using a simultaneous equation subroutine on Eqs. (4), the coefficients B_ℓ are solved. One of the computer subroutines performs the operation of reading in measured feed pattern values then solving for the coefficients B_ℓ and storing them. Another subroutine can then be called whenever needed to calculate the feed pattern from Eq. (3).

For regions of the feed pattern where there is ripple or low values a piece-wise linear approximation is used. One subroutine calculates the slope of each section as shown in Fig. 11 from

$$(5) \qquad \left.\frac{\Delta f}{\Delta \psi}\right|_{\psi_i} = \frac{f(\psi_{i+1}) - f(\psi_i)}{\psi_{i+1} - \psi_i} \quad .$$

Another subroutine can then be called when needed to calculate the feed pattern in the piece-wise linear region from

$$(6) \qquad f(\psi) = f(\psi_i) + \left.\frac{\Delta f}{\Delta \psi}\right|_{\psi_i} (\psi - \psi_i)$$

for $\psi_i \leq \psi \leq \psi_{i+1}$.

A result using the combination of polynomial-fit and piece-wise linear approximation on a symmetrical sum pattern (even terms only) is shown in Fig. 12. The polynomial fit was used for $0 \leq \psi \leq 85°$, and the piece-wise linear approximation was used for $85° \leq \psi \leq 180°$.

Although GTD can be used to calculate most of the far field pattern, the main beam and near sidelobes of the reflector antenna will be calculated by the aperture integration approach. Since the required integration is usually very cumbersome for electrically large antennas, an approach based on using overlapping rectangular subapertures is being used. Each subaperture can be electrically large, i.e., several wavelengths in size. This will minimize the number of subapertures required.

Preliminary results have been obtained using this aperture integration approach for a line source with an exactly known far field pattern as a check case. It was found that the use of overlapping rectangular subapertures each with a triangular subaperture distribution gives excellent accuracy with relatively few aperture field samples. The aperture distribution for the line source used in the check case is shown in Fig. 13. A spacing of 2λ was used between "sample" points along the 20λ aperture. As seen from Fig. 13 the overlapping subapertures (triangular distribution) give a good piece-wise linear approximation to the 20λ aperture distribution. The use of non-overlapping subapertures each with a uniform distribution also is shown in Fig. 13; this technique gives a "step" approximation and thus requires considerably more "sample" points than the use of the overlapping subaperture to achieve the same accuracy. The exact far field pattern is shown in Fig. 14 along with
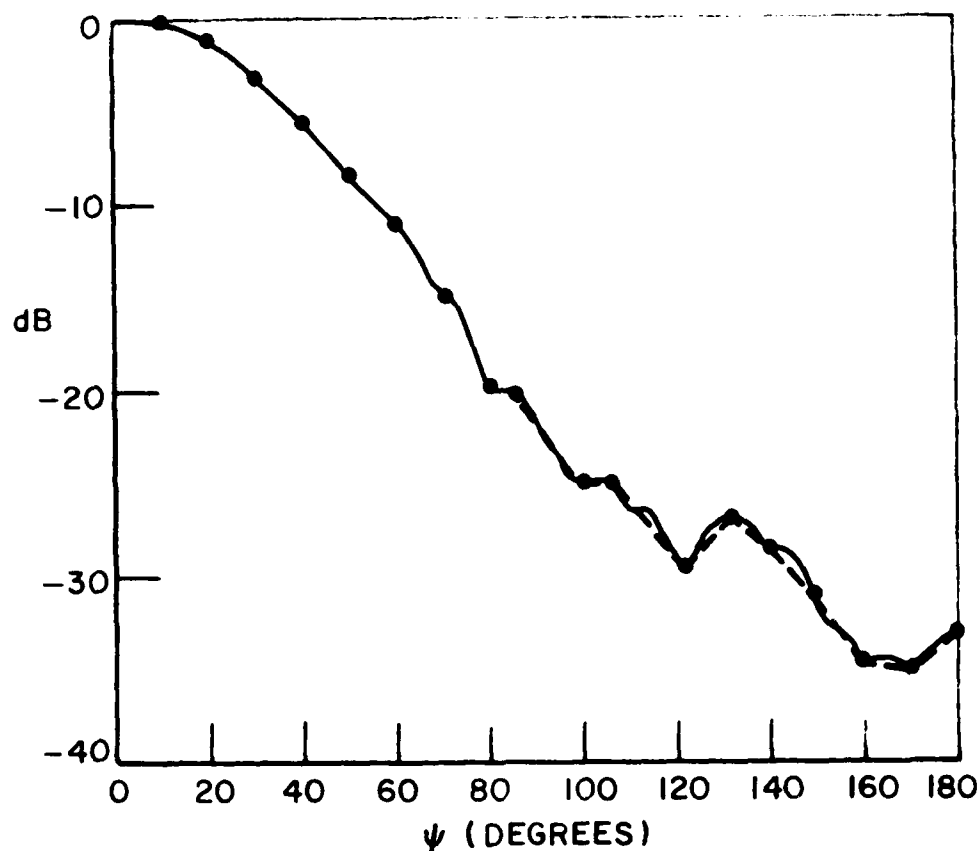
18

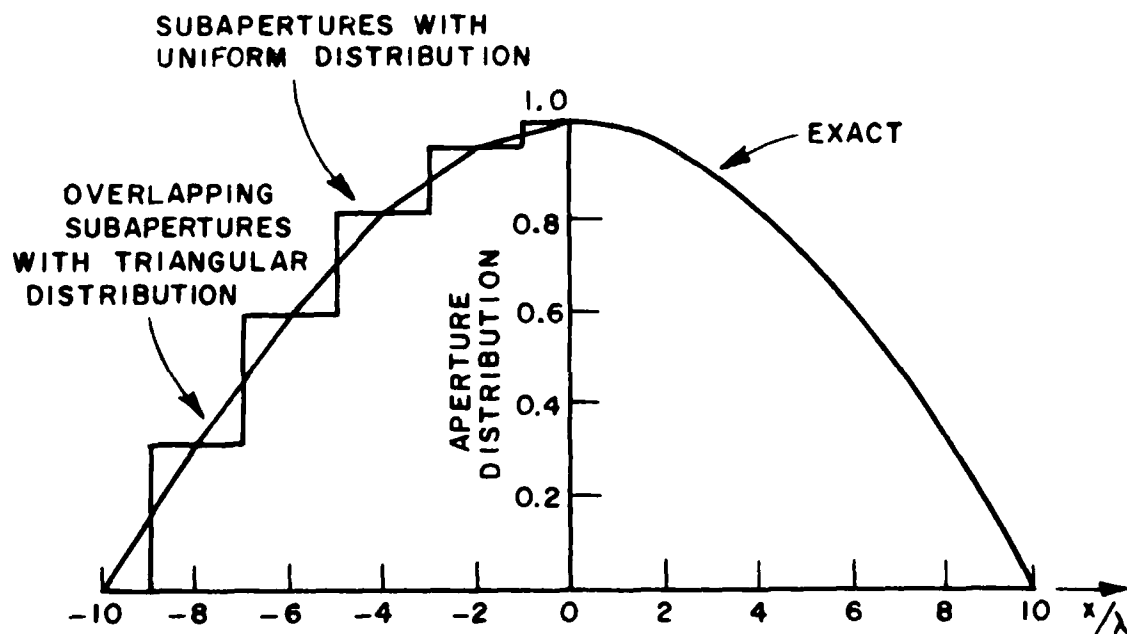Fig. 12. Measured feed pattern and its analytic fit.

Fig. 13. Exact aperture distribution and approximation
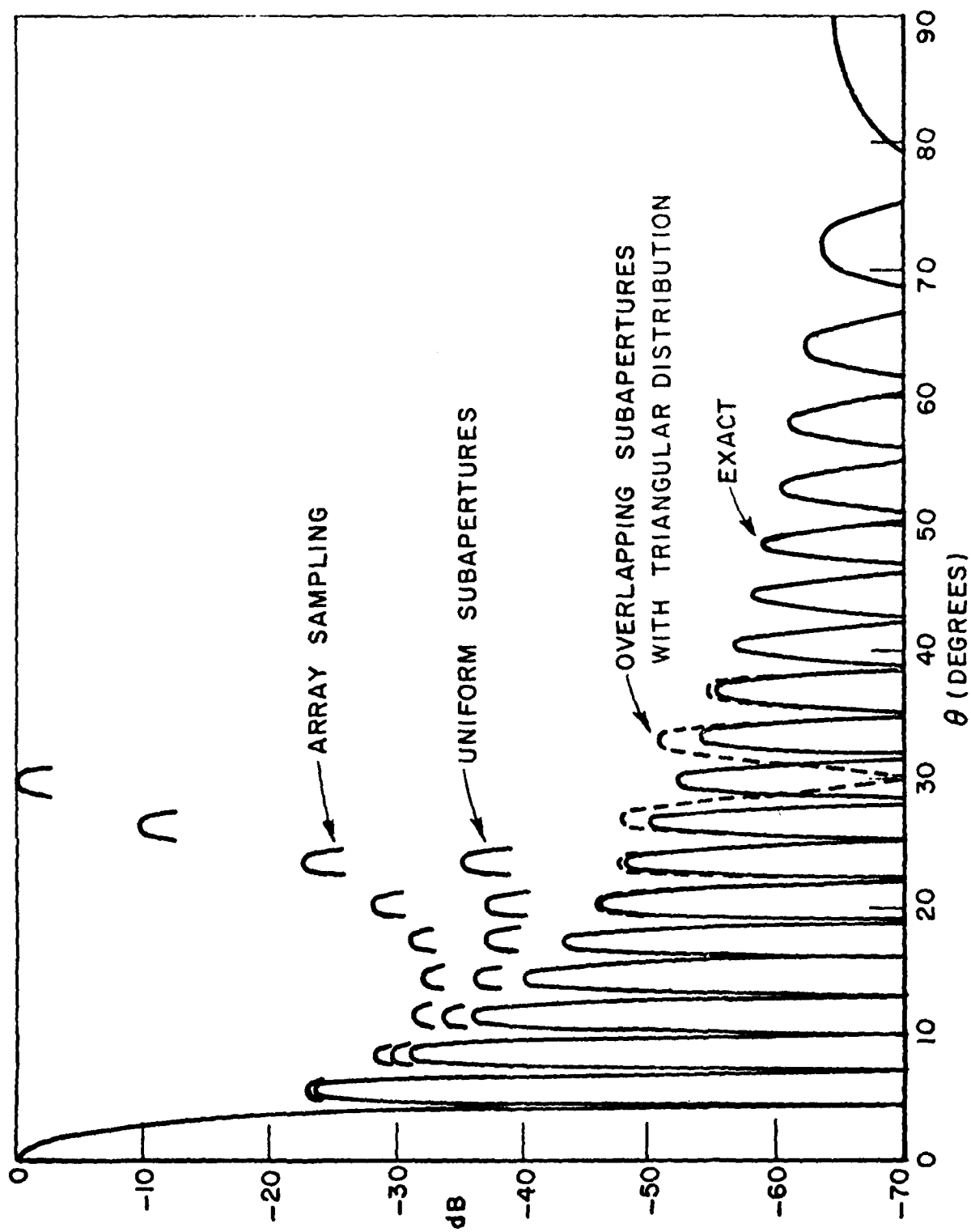to it by subaperture techniques.

19

Fig. 14. Exact far field pattern and calculations based on subaperture techniques.

patterns calculated from the overlapping subapertures (triangular dis-
tribution) and non-overlapping subapertures (uniform distribution).
The result using "array" sampling is also shown in Fig. 14. The rec-
tangular subapertures with triangular distribution appear to be superior
to other aperture integration methods such as "array" sampling of the
aperture field or rectangular subapertures with uniform distributions
and will be incorporated into our general reflector code.

V. THEORETICAL STUDIES

Edge diffraction is part of the foundation of the Geometrical
Theory of Diffraction (GTD). A uniform solution for the diffraction of
an electromagnetic wave by a perfectly conducting wedge has been obtained
within the format of the GTD. If the field incident on the edge does
not have a rapid spatial variation, the diffracted field is directly
proportional to the incident field at the edge and it can be calculated
using the dyadic diffraction coefficient given by Kouyoumjian and Pathak
[1].

In many practical problems, however, the incident field has rapid
spatial variation at a diffracting edge. If the edge diffracted field
is calculated in the usual way[1] there will be a discontinuity in the
spatial derivatives of the total field, i.e., the calculated pattern
will be continuous but have a "kink" in it. Some examples were given
in the previous report[2].

Thus, the theoretical studies on this contract to date have con-
centrated on the development of an accurate yet simple slope-diffraction
coefficient. Some details were given in the previous report[2]. This
study is essentially completed and full details will be presented in a
technical report that is in preparation. Numerical examples will be
included to illustrate the usefulness of slope diffraction.

REFERENCES

[1]   R.G. Kouyoumjian and P.H. Pathak, "A Uniform Geometrical Theory
      of Diffraction for an Edge in a Perfectly Conducting Surface,"
      Proc. IEEE, Vol. 62, November 1974, pp. 1448-1461.

[2]   R.G. Kouyoumjian, R.J. Marhefka, R.C. Rudduck and C.H. Walter,
      "Asymptotic High Frequency Techniques for UHF and Above Antennas,"
      Report 4508-1, November 1976, The Ohio State University Electro-
      Science Laboratory, Department of Electrical Engineering; prepared
      under Contract N00123-76-C-1371 for Naval Regional Procurement
      Office.

END

FILMED

9-83

DTIC